

Dielectric Relaxation Spectroscopy of Gradient Copolymers and Block Copolymers: Comparison of Breadths in Relaxation Time for Systems with Increasing Interphase

Michelle M. Mok,[†] Kevin A. Masser,[‡] James Runt,^{*,‡} and John M. Torkelson^{*,§,†}

[†]Department of Materials Science and Engineering, Northwestern University, Evanston, Illinois 60208,

[‡]Department of Materials Science and Engineering, The Pennsylvania State University, University Park, Pennsylvania 16802, and [§]Department of Chemical and Biological Engineering, Northwestern University, Evanston, Illinois 60208

Received April 6, 2010; Revised Manuscript Received May 21, 2010

ABSTRACT: Two series of styrene/*n*-butyl acrylate (S/*n*BA) gradient copolymers and block copolymers are prepared with a range of molecular weights to investigate the effect of increasing interphase on relaxation time distributions and to relate these to measurements of glass transition breadth using differential scanning calorimetry and dielectric relaxation spectroscopy (DRS). This is the first time DRS has been used in the study of gradient copolymers. The segmental relaxation associated with the dielectrically active component of the block copolymers (*n*BA) resembles that of poly(*n*-butyl acrylate) in behavior but becomes broader as the system shifts from highly segregating to moderately segregating. In contrast, the gradient copolymer segmental relaxation largely resembles that of a random copolymer with similar composition but with broader relaxation time distributions. The one exception is the most phase-segregated of the gradient copolymers, for which the relaxation response appears as two overlapping contributions representing regions of high *n*BA content and low *n*BA content. The breadth in relaxation time achieved by this gradient copolymer is comparable to or exceeds that of a weakly segregated block copolymer.

1. Introduction

Gradient copolymers are a type of linear copolymer where the comonomer composition varies smoothly throughout the length of the chain, from mostly A-monomer to mostly B-monomer.^{1–3} This gradual change in comonomer composition in comparison to block copolymers has inspired studies of gradient copolymer phase separation. In separate publications, Lefebvre et al.⁴ and Jiang et al.⁵ used self-consistent mean-field (SCMF) theory to calculate phase diagrams of phase segregated gradient copolymers with differing gradient sequences and also their equilibrium composition profiles at different segregation strengths. Both groups predicted that gradient copolymers phase segregate to yield approximately sinusoidal composition profiles that grow in compositional amplitude with increasing values of χN (where χ is the Flory–Huggins interaction parameter and N is the chain length). This indicates that gradient copolymers should exhibit behavior reflecting a range of compositions from A-rich to B-rich rather than simply the pure-A and pure-B compositions observed in phase separated block copolymers.

Experimental evidence of such properties has been found in studies of glass transition temperature (T_g) breadth by differential scanning calorimetry,^{6–14} dynamic mechanical analysis^{1,8,9,15,16} and ellipsometry.¹⁷ These revealed extremely broad glass transition regions for gradient copolymers compared to homopolymers and random copolymers, i.e., 70–80 °C for a styrene/4-hydroxystyrene gradient copolymer compared to 14–17 °C for a random copolymer of the same copolymer system.¹² Generally, in strongly segregating systems, very broad glass transitions spanning more than 70% of the difference between the homopolymer T_g s were

observed, whereas in moderately segregating systems, much more variable T_g breadths were observed, with strong dependence on copolymer architecture.¹⁴

It is of significant interest to the polymer community to determine whether these broad transition temperature ranges can be directly related to measured breadths in relaxation time. As stated by Graham Williams in 2009: “In addition to further [broadband dielectric spectroscopy (BDS)] studies along current themes, many new developments of BDS can be envisaged including, e.g., studies of chain dynamics in bulk samples of “gradient” copolymers, to reveal the molecular origins of their exceptionally broad glass transition regions...”¹⁸ Here, we employ dielectric relaxation spectroscopy (DRS = BDS) to examine the relaxation properties of gradient copolymers over a large frequency range. This technique measures the relaxation of dipoles under an oscillating electric field; the time scales of these relaxations correlate to cooperative segmental or subsegmental dynamics of the polymer. A large range of time scales, and hence length scales, can be probed as the frequency is changed over many orders of magnitude, nine or more in some cases.^{19–21} Dielectric relaxation spectroscopy can detect not only the slower α -relaxations, which are ascribed to T_g -related cooperative segmental motion, but also the faster β - and γ -relaxations (where they exist) which are ascribed to side group motion or other local system-specific behaviors.

Dielectric relaxation spectroscopy is extensively used to compare the influence of polymer architecture and the addition of secondary species on both the location and breadth of the relaxation processes. For example, it has been used to study the broadening compared to random copolymers and homopolymers of the α -relaxation peak in polymer blends,^{22–29} interpenetrating polymer networks³⁰ and for polymers with small-molecule additives.³¹ This broadening has been attributed to a range of

*To whom correspondence should be addressed. E-mail: (J.R.) runt@matse.psu.edu; (J.M.T.) j-torkelson@northwestern.edu).

local environments.^{23,32,33} In block copolymer systems, DRS has been used primarily to study diblock, multiblock and star copolymers of the styrene-isoprene comonomer system.^{34–40} These include examination of block dynamics near the order–disorder transition^{34–36} as well as determining interfacial widths in phase-segregated systems where mobile isoprene midblocks are anchored by glassy styrene end-blocks.^{37–40}

The DRS technique has also been extended to study the effects of free surfaces and interfacial interactions on the dynamics of confined polymers. In nanoconfined geometries such as thin films or nanocomposites, the fraction of polymer material near a surface or an interface grows to become significant in relation to the fraction of “bulk” material, similar to the enhanced presence of interphase compositions in gradient copolymers. Relative to their bulk behavior, segmental mobilities are enhanced at free surfaces and may be diminished at material interfaces (determined by the available interactions), leading to a range of possible T_g s and relaxation rates depending on the system geometry.^{41–46} In DRS studies of ultrathin films and nanocomposites, confinement effects appear as α -relaxation peak shifts and α -relaxation peak broadening,^{47–49} β -relaxation peak diminishment⁵⁰ and the appearance of additional cooperative or noncooperative peaks.^{48,51}

Here, DRS is applied for the first time to characterize gradient copolymer dynamics; in particular, a set of styrene/*n*-butyl acrylate (S/nBA) block and gradient copolymers are used to examine the effects of polymer architecture and phase segregation on relaxation time breadths. This copolymer system was chosen due to the large difference in the mobilities of its homopolymer components, setting up the potential for very broad relaxations. Its moderate segregation strength (the Flory–Huggins interaction parameter (χ) for S/nBA has been reported as 0.034⁵² as well as 0.087⁵³) makes the overall level of phase segregation in the gradient copolymers highly tunable.¹⁴ The dipole moment of nBA units is also far greater than that of styrene units, which makes it possible to probe the response of essentially only one of the components; such specificity has not been possible in any other technique used to study gradient copolymers.

Two sets of S/nBA copolymers designed to present increasing amounts of interphase are investigated. The first set is a series of block copolymers with decreasing molecular weight, ranging from strongly segregated (i.e., very narrow interfaces between the pure styrene and pure nBA regions) to moderately segregated (broader interfaces). The second set is a series of gradient copolymers with increasing molecular weight; this should lead to an increasing degree of phase segregation, pushing the sinusoidal composition profiles associated with nanophase segregated gradient copolymers to increasing amplitudes or broader ranges of compositions.^{4,5} The relaxation breadths and behavior of these two series will be compared against each other as well as against those of PnBA and an S/nBA random copolymer.

2. Experimental Section

2.1. Materials and Methods. The nomenclature employed for the copolymers throughout this work is S-*rand*-nBAXX, S-*block*-nBAXX and S-*grad*-nBAXX for random, block, and gradient copolymers, respectively, where XX is a number representing the cumulative styrene mole composition as determined from ¹H NMR.

The PnBA homopolymer was prepared using nitroxide-mediated controlled radical polymerization (NM-CRP) from BlocBuilder initiator (*N*-(2-methylpropyl)-*N*-(1-diethylphosphono-2,2-dimethylpropyl)-*O*-(2-carboxylprop-2-yl) hydroxylamine, 99%) which was kindly supplied by Arkema, Inc. and is the same material as that used by Lessard et al.,^{54,55} Eggenhuisen et al.⁵⁶ and Dire et al.⁵⁷ The reaction was carried out at an initiator concentration of 1.88×10^{-3} mol/L for 6.0 h at 100 °C. In all polymerizations, the test tube contents were

purged with N₂ for 30 min prior to reaction. Its molecular weight ($M_n = 155K$) was determined by gel permeation chromatography (GPC, Waters Breeze) with tetrahydrofuran as the eluent using universal calibration with PS standards.

The S/nBA random copolymer (S-*rand*-nBA55, $M_n = 95K$) was synthesized using conventional free radical polymerization from 2,2'-azobis(isobutyronitrile) (Pfaltz and Bauer). The reaction was carried out at an initiator concentration of 1.35×10^{-2} mol/L in 47:53 S:nBA for 20 min at 70 °C. The reported molecular weight is an apparent molecular weight measured relative to PS standards.

Three S/nBA block copolymers were synthesized using sequential NM-CRP, starting from PS macroinitiators prepared from BlocBuilder. The two cases with moderate molecular weight were extended from the same macroinitiator ($M_n = 32K$) to yield S-*block*-nBA81 ([PS] = 3.87×10^{-3} mol/L for 1.0 h at 90 °C, $M_n = 41K$) and S-*block*-nBA68 ([PS] = 3.79×10^{-3} mol/L for 1.0 h at 100 °C, $M_n = 51K$), and a high molecular weight case was prepared from a macroinitiator with $M_n = 71K$ to yield S-*block*-nBA23 ([PS] = 1.14×10^{-3} mol/L for 6.0 h at 100 °C, $M_n = 364K$). The block copolymer molecular weight values were calculated from the M_n of the PS macroinitiators and their final comonomer compositions as measured by ¹H NMR. For the remainder of this work, these will be referred to as S-*block*-nBA81–41K, S-*block*-nBA68–51K, and S-*block*-nBA23–364K.

Three gradient copolymers of similar nBA content but increasing molecular weight were prepared using semibatch NM-CRP from the initiator alkoxyamine 29 (2,2,5-trimethyl-3-(1-phenylethoxy)-4-phenyl-3-azahexane⁵⁸): S-*grad*-nBA60–72K, S-*grad*-nBA60–95K and S-*grad*-nBA61–152K. In each case, nBA was continuously added to a test tube of styrene to create the gradient effect. The reported molecular weights are apparent molecular weights measured relative to PS standards. The S-*grad*-nBA60–72K case was synthesized from an initiator concentration of 3.92×10^{-3} mol/L in 10 mL styrene for 8.0 h at 100 °C, with nBA being added at 3 mL/h throughout the polymerization. The S-*grad*-nBA60–95K and S-*grad*-nBA61–152K synthesis conditions were fully described in a previous publication.³

2.2. Differential Scanning Calorimetry. Thermal analysis was done with a differential scanning calorimeter (Mettler-Toledo DSC 822e) calibrated with indium and zinc standards. Dry N₂ was passed through the DSC cell during measurement. Samples were heated to at least 30 °C above their component T_g s and held at that temperature for 30 min to erase thermal history (first heat). Each sample was then cooled below its component T_g s at a rate of 40 °C/min and reheated at a rate of 10 °C/min (second heat). Glass transition breadth data were extracted from the second heat scan. All measurements were repeated twice.

2.3. Dielectric Relaxation Spectroscopy. All samples were dissolved in tetrahydrofuran and filtered through a 0.2 μ m syringe filter to remove impurities and cast into Teflon containers. The solvent was allowed to slowly evaporate at room temperature and then dried further overnight under vacuum at least 30 °C above the sample T_g as measured by DSC. The rubbery PnBA sample was deposited directly onto brass electrodes for measurement and fused silica fibers 50 μ m in diameter were used as spacers to fix the sample thickness. All the S/nBA copolymer samples were hot-pressed between two metal plates, with Kapton film as an intermediary layer, at a temperature 30 °C above their T_g end point by DSC. The samples were allowed to sit on the press for 2 min to heat before 0.5 ton of pressure was applied and held for 15 min to yield roughly circular films 100–200 μ m in thickness and exceeding 20 mm in diameter. The pressed films were further heated in vacuum overnight to remove any remaining solvent and residual stress. Finally, gold (~100 nm) was sputtered onto each side of the sample to enhance contact with the brass electrodes.

Isothermal dielectric spectra were collected using a Novocontrol GmbH Concept 40 broadband dielectric spectrometer over

Table 1. Molecular Characterization of S/nBA Copolymers

| sample | M_n (g/mol) | F_S |
|-----------------------------|----------------------|-------|
| PnBA | 155 000 ^a | |
| S- <i>block</i> -nBA23–364K | 364 000 ^c | 0.23 |
| PS macroinitiator | 71 000 ^b | |
| S- <i>block</i> -nBA68–51K | 51 000 ^c | 0.68 |
| PS macroinitiator | 32 000 ^b | |
| S- <i>block</i> -nBA81–41K | 41 000 ^c | 0.81 |
| PS macroinitiator | 32 000 ^b | |
| S- <i>rand</i> -nBA55 | 95 000 ^b | 0.55 |
| S- <i>grad</i> -nBA60–72K | 72 000 ^b | 0.60 |
| S- <i>grad</i> -nBA60–95K | 95 000 ^b | 0.60 |
| S- <i>grad</i> -nBA61–152K | 152 000 ^b | 0.61 |

^a Characterized using universal calibration with PS standards by GPC with THF as eluent. ^b Characterized relative to PS standards by GPC with THF as eluent. ^c M_n value was determined from the M_n of PS macroinitiator and the F_S value.

the frequency range 0.01 Hz to 10 MHz. Measurements were taken on heating. Temperature was controlled by a Novocontrol Quatro Cryosystem, which uses N₂ to heat and cool the sample and has a stability of ± 0.1 °C. Measurements of the block copolymers and PnBA were taken to temperatures as low as -150 °C, while those for the random copolymer and the gradient copolymers were taken as low as -100 or -140 °C.

Relaxation times (τ_{\max}) were obtained by fitting the isothermal dielectric loss spectra to the sum of a Havriliak–Negami (HN) function⁵⁹ and a dc loss contribution:

$$\epsilon''(\omega) = -\frac{\Delta\epsilon}{(1+(\omega\tau)^\alpha)^\gamma} + \frac{\sigma_0}{\epsilon_0\omega^s} \quad (1)$$

where $\Delta\epsilon$ is the dielectric strength, ω is the angular frequency, τ is the characteristic relaxation time, α and γ are shape parameters related to the breadth and symmetry, σ_0 is the dc conductivity (S/cm), ϵ_0 is the permittivity of vacuum, and s characterizes the type of conduction ($s \leq 1$).

A few of the isothermal data exhibited a small temperature-independent contribution associated with the sputtered electrodes. These were fitted with an HN function and removed from the data.

3. Results and Discussion

3.1. Characterization of Copolymers and Copolymer Glass Transition Breadths. The molecular weight and comonomer composition characterizations of the PnBA homopolymer, the random S/nBA copolymer, three S/nBA block copolymers and three S/nBA gradient copolymers are summarized in Table 1. The series of three block copolymers are of increasing molecular weight ($M_n = 41$ K, 51K, 364K) and decreasing cumulative styrene fraction ($F_S = 0.81, 0.68, 0.23$). The series of three gradient copolymers are of increasing molecular weight ($M_n = 72$ K, 95K, 152K) and extremely similar cumulative styrene content ($F_S = 0.60, 0.60, 0.61$). The random copolymer has a styrene content comparable to the gradient copolymers ($F_S = 0.55$).

The derivative DSC heat flow curves for all the samples are shown in Figure 1. In these derivative curves, glass transitions appear as easily discernible peaks rather than the step-functions found in typical heat flow curves.^{12–14} The homopolymer and block copolymer responses are shown in Figure 1(a). Poly(*n*-butyl acrylate) exhibits a single, sharp peak at -48 °C, consistent with the T_g of this polymer. The two higher molecular weight block copolymers display two distinct responses, one near the PnBA T_g (~ -55 °C) and another near the PS T_g (~ 100 °C). The nBA block-related peaks all exhibited maxima at -48 °C, while the styrene block response shifted from 104 °C for the high molecular

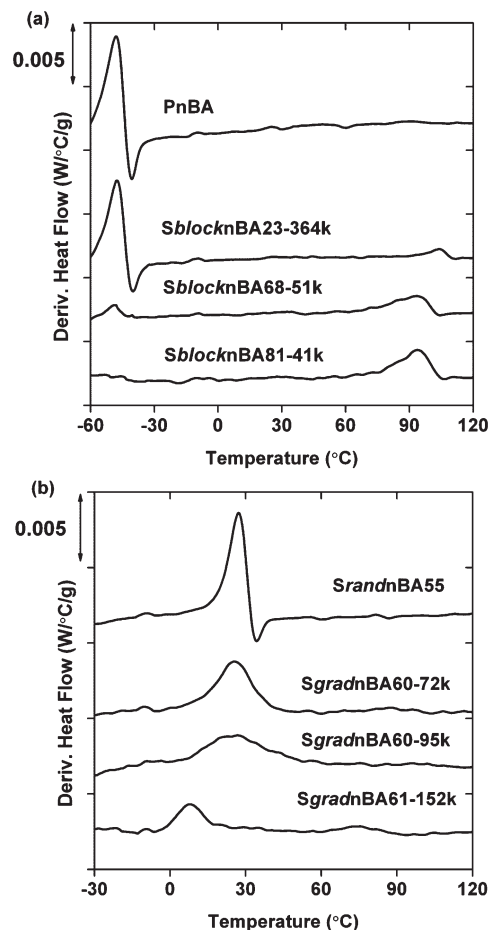


Figure 1. (a) Derivative DSC heat flow curves for PnBA and S/nBA block copolymers. (b) Derivative DSC heat flow curves for S/nBA random copolymer and gradient copolymers.

weight case (S-*block*-nBA23–364K) to 94 °C for the moderate molecular weight case (S-*block*-nBA68–51K); the 51K copolymer response is also broader than that of the 364K copolymer. This reflects the reduced degree of phase segregation that is induced by the decreasing molecular weight of the system, with the 51K case being only moderately segregated ($\chi N = \sim 16$ –40) while the 364K case is strongly segregating ($\chi N = \sim 100$ –270) (using χ values reported in the literature^{52,53}). The relative magnitude of the two transitions in each block copolymer also changes to reflect the relative comonomer compositions, as expected. The lowest molecular weight case (S-*block*-nBA81–41K) shows no indication of a response near the nBA block T_g , but a broad response is seen corresponding to the styrene-block T_g (at 94 °C). Since the value observed for the styrene-block T_g matches with that of the S-*block*-nBA68–51K case, this suggests that the system is phase-segregated rather than phase-mixed, but that there is too little of the segregated nBA-block to generate an observable signal by DSC. In contrast, DSC measurements by Miwa et al.⁶⁰ of a phase-mixed S/nBA block copolymer showed significant shifts in the glass transition region compared to a phase-segregated case.

Figure 1b shows the DSC derivative results for the random copolymer and the three gradient copolymers. The random copolymer shows a single, narrow glass transition region ($\Delta T_g = 19$ °C) with the peak at 28 °C; this is consistent with its composition¹⁴ ($F_S = 0.55$). The three gradient copolymers exhibit single glass transition regions which broaden with increasing molecular weight, from 30 °C in breadth for the $M_n = 72$ K case,

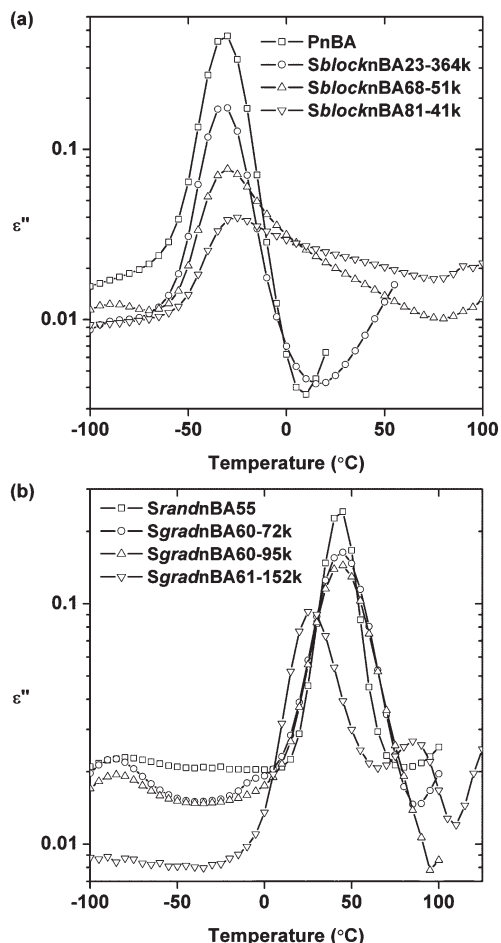


Figure 2. (a) Isochronal dielectric loss results for PnBA and S/nBA block copolymers at 100 Hz. (b) Isochronal dielectric loss results for S/nBA random copolymer and gradient copolymers at 100 Hz. Solid lines serve as a guide for the eye.

to 54 °C for the 95K case and finally 90 °C for the 152K case. This reflects the increasing χN value of the system, which should increase the amplitude of the phase-segregated sinusoidal composition profiles.

We can compare these results with isochronal measurements (constructed for $f = 100$ Hz) of the copolymer dielectric responses as a function temperature (Figure 2). Since the strength of the dielectric response of styrene units is negligible because of their very low dipole moment,⁵⁰ effectively all of the dielectric response arises from the nBA units. The PnBA homopolymer and the S/nBA block copolymers are compared in Figure 2a. Over this temperature range, the PnBA sample shows a relatively strong and narrow process centered at -33 °C, with the suggestion of a weaker response immediately adjacent at lower temperatures. This principal relaxation is the segmental (α) process for segments with nBA units. The weak lower temperature process has very similar characteristics and is in the same temperature and frequency range as a relaxation observed in a wide variety of polymeric systems containing water,^{61,62} and this will not be discussed further.

Each of the S/nBA block copolymers also exhibits a single strong relaxation near the T_{α} of PnBA, with decreasing strength as styrene content is increased. The response for the S-block-nBA23-364K sample remains narrow, but those for the other two block copolymers are significantly broadened toward higher temperatures, yielding broad glass transition ranges. Overall, it appears that the motions of

the nBA segments are being hindered by the presence of the styrene-blocks. At these molecular weights, there could be significant intramolecular effects, similar to those previously studied in block copolymers by DRS,³⁷⁻⁴⁰ due to their covalent attachment to the glassy styrene blocks. Another possibility is intermolecular effects, with greater interpenetration of the styrene and nBA chains. This is consistent with their lower molecular weights and the higher fraction of interphase that this would impart, as these interphase regions would be of higher styrene content.

Figure 2b compares the isochronal DRS results constructed at 100 Hz for the random copolymer and the three gradient copolymers. The random copolymer exhibits a single sharp relaxation centered at 40 °C at this frequency, associated with the segmental relaxation of this material; it is similar in breadth to the segmental process of PnBA, but reduced in strength, reflecting the reduction in nBA content.⁶³ The S-grad-nBA60-72K and S-grad-nBA60-95K copolymers exhibit slightly broader relaxations centered at 45 °C. This increase in breadth and shift to a slightly higher temperature are consistent with the DSC data. For the S-grad-nBA61-152K copolymer, a much broader, multimodal temperature response is observed with a strong relaxation centered at 25 °C and a weaker process at about 70 °C. This is consistent with phase separation of the gradient copolymer into styrene-rich and nBA-rich regions within a sinusoidal composition profile, and a stronger relaxation would be expected in the nBA-rich region owing to the difference in dielectric activities of S and nBA. The isochronal temperature breadth for its α -relaxation process by DRS is consistent with the extreme breadth observed by DSC.

3.2. Segmental Relaxation Spectra. Figures 3 and 4 show the dielectric loss spectra for all the polymers plotted as a function of frequency at temperatures associated with the segmental relaxation of the nBA-rich phase. In Figure 3, the plots associated with the PnBA homopolymer and the three block copolymers are shown over temperatures from -50 to 10 °C. At -50 °C for PnBA, the α relaxation of PnBA is just emerging at low frequencies and shifts to higher frequencies with increasing temperature. For each of the block copolymers, a similar relaxation is evident at the same frequencies for the same temperatures as PnBA, consistent with the response originating from phase segregated, nBA-rich regions. There is a pronounced asymmetry of the relaxation to low frequencies, reflecting the previous conjecture of intramolecular or intermolecular effects hindering the motions of the nBA chains. As shown in Figure 5, the measured relaxation strengths diminish significantly with decreasing nBA content.

In parts a-d of Figure 4, the dielectric loss spectra for the random copolymer and the three gradient copolymers are shown over temperatures from 20 to 80 °C. In the random copolymer case, the segmental process is seen at low frequencies at 30 °C, and shifts to higher frequencies with increasing temperature. The two lower molecular weight gradient copolymers (S-grad-nBA60-72K and S-grad-nBA60-95K) exhibit slightly broader relaxations and are shifted to higher frequencies by one decade at equivalent temperatures. This shift in frequency is likely associated with the difference in composition, with the random copolymer ($F_S = 0.55$) having lower styrene content than both gradient copolymers ($F_S = 0.60$). In the high molecular weight gradient copolymer (S-grad-nBA61-152K), the location at equivalent temperatures is shifted to yet higher frequencies. Also, a much smaller contribution to the loss is noticeable at temperatures above 50 °C at frequencies slightly lower than the α process. On the basis of its location, this contribution is

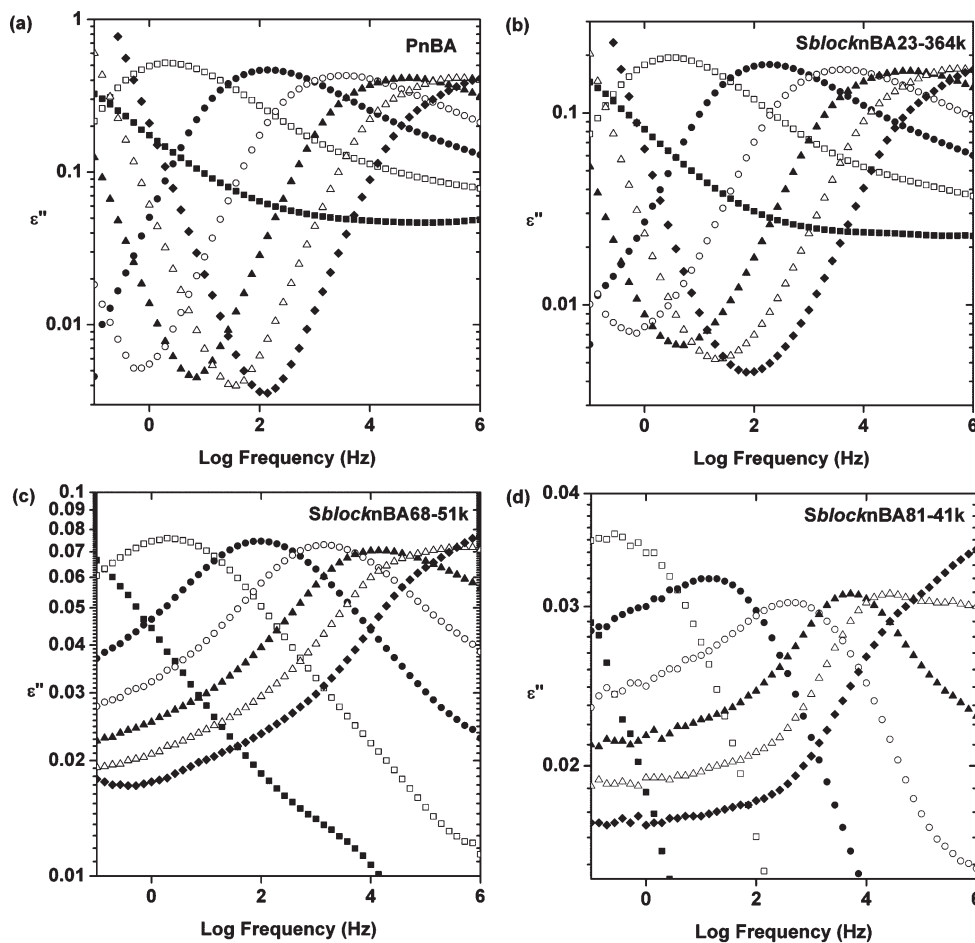


Figure 3. Dielectric loss spectra for (a) PnBA (b) *S-block-nBA*23–364K (c) *S-block-nBA*68–51K and (d) *S-block-nBA*81–41K at $-50\text{ }^{\circ}\text{C}$ (■), $-40\text{ }^{\circ}\text{C}$ (□), $-30\text{ }^{\circ}\text{C}$ (●), $-20\text{ }^{\circ}\text{C}$ (○), $-10\text{ }^{\circ}\text{C}$ (▲), $0\text{ }^{\circ}\text{C}$ (Δ), and $10\text{ }^{\circ}\text{C}$ (◆).

proposed to arise from nBA units in the styrene-rich regions, which were shown earlier to exhibit a T_g at $\sim 70\text{--}80\text{ }^{\circ}\text{C}$.

Also worth noting from Figures 3 and 4 is the difference in curve-shapes between the different polymer types. The PnBA homopolymer, *S/nBA* random copolymer and the block copolymers all exhibit the usual Kohlrausch–Williams–Watts stretched exponential line-shapes. Meanwhile, the gradient copolymers exhibit more symmetric Cole–Cole-type relaxation peaks, reflecting the sinusoidal composition profiles expected in their phase segregated state.

Figure 6 shows dielectric loss spectra normalized to both ϵ''_{max} and f_{max} for the segmental process of the copolymers. In parts a and b of Figure 6, temperatures were chosen such that f_{max} of the α process was closest to 100 Hz. Figure 6a shows the normalized curves for the PnBA homopolymer and the three block copolymers. The *S-block-nBA*23–364K case exhibits a transition only very slightly broadened compared to the PnBA homopolymer. With decreasing molecular weight, the two other block copolymer cases show increasingly broadened transitions. This can be ascribed to the increased proportion of interphase.

In Figure 6b, the normalized loss curves for the random copolymer and the three gradient copolymers are shown. All three of the gradient copolymers exhibit significantly broader relaxation responses compared to the random copolymers. The two gradient copolymers with lower molecular weight (*S-grad-nBA*60–72K and *S-grad-nBA*60–95K) exhibit slightly broader responses than the highest molecular weight case (*S-grad-nBA*61–152K). The lower molecular weight gradient

copolymers have a greater extent of mixing than *S-grad-nBA*61–152K, and they have a broader transition in the frequency/temperature range of Figure 6b. As seen in Figure 2, *S-grad-nBA*61–152K exhibits two α processes, with $\sim 45^{\circ}$ between the maxima. The data for *S-grad-nBA*61–152K in Figure 6(b) is only representative of the α relaxation of the nBA rich phase, and should be relatively “narrow”. The total segmental relaxation time distribution for this copolymer is, however, exceptionally broad.

Since the dielectric loss spectra of *S-grad-nBA*61–152K at temperatures exceeding $50\text{ }^{\circ}\text{C}$ appeared to include a secondary process (Figure 4d), we also compare the normalized responses of the random and gradient copolymers where f_{max} of the segmental process was closest to 1 MHz (Figure 6c). At temperatures corresponding to this f_{max} , the behavior at much lower frequencies relative to the primary process can be observed. In the *S-grad-nBA*60–72K and *S-grad-nBA*60–95K cases, a broadening at low frequencies is observed from the random copolymer case. In the *S-grad-nBA*61–152K case, a primary process can be observed with broadening similar to the lower molecular weight gradient cases, but now a secondary, weaker contribution is apparent at lower frequencies, as the magnitude of the normalized loss response in this region is significantly higher for this case than the random copolymer case and the other two gradient copolymer cases. This secondary contribution appears at a frequency consistent at this temperature with the styrene-rich region contribution observed in the isochronal data and DSC data, and makes the total segmental

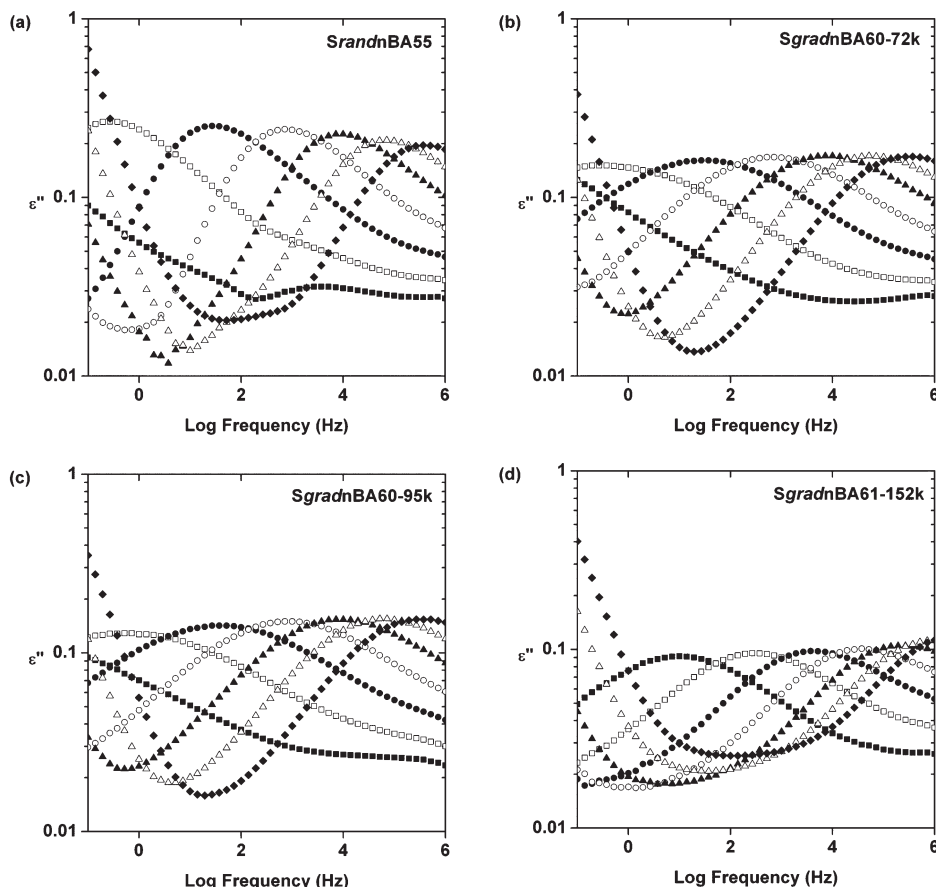


Figure 4. Dielectric loss spectra for (a) SrandnBA55 (b) S-grad-nBA60–72K (c) S-block-nBA60–95K and (d) S-block-nBA61–152K at 20 °C (■), 30 °C (□), 40 °C (●), 50 °C (○), 60 °C (▲), 70 °C (△) and 80 °C (◆). The significant upturn in the loss at low frequencies and higher temperatures arises from dc conduction of ionic impurities.

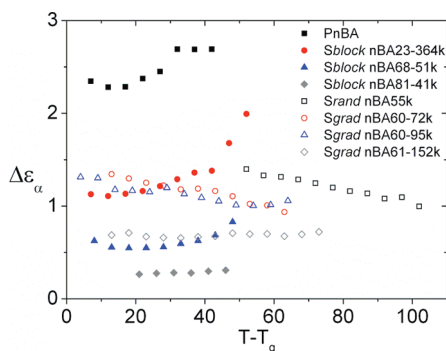


Figure 5. Measured relaxation strengths for the α process as a function of $T - T_g$.

relaxation time distribution for this copolymer exceptionally broad.

3.3. Characterization of Relaxation Times. The average relaxation times $\tau = 1/(2\pi f)$ associated with the segmental processes were extracted from isochronal data and plotted in an Arrhenius diagram as a function of reciprocal temperature (Figure 7). These were checked against the shift in peak values obtained from fitting HN functions to isothermal results (for a frequency range of 0.01 Hz to 10 MHz) and found to overlap. Although not shown in Figure 7, we also observed a low-strength, local process ($E_a \sim 20$ kJ/mol) at lower temperatures (~ -130 to -150 °C or $1000/T = \sim 7-8$ K $^{-1}$), associated with local motion in the nBA units, as observed previously by others.^{64–66} Hayakawa and Adachi⁶⁵

asserted that the process was of too low a strength for an ester group rotation and so designated it as a “ γ -relaxation” (presumably associated with *n*-butyl units).

The data in Figure 7 at values of $1000/T$ between 3.5 and 4.5 corresponds to PnBA and the block copolymers, where the observed relaxation is associated with pure or near-pure nBA regions. Data from all of these samples essentially overlap at higher values of $1000/T$, supporting the assertion made earlier that all the block copolymers are phase-segregated into essentially pure-nBA regions. The small shift in behavior for S-block-nBA81–41K at lower values of $1000/T$ may indicate that some temperature-dependent phase mixing is occurring at higher temperatures.⁶⁰

The second set of segmental processes located at values of $1000/T$ below 3.5 corresponds to the random copolymer and gradient copolymers, where the higher characteristic temperatures reflect the mixing of styrene and nBA units. The data for the random copolymer, S-grad-nBA60–72K and S-grad-nBA60–95K overlap, but that associated with S-grad-nBA61–152K are slightly removed from the others in this set to higher $1000/T$ values. This reflects the observations noted regarding its dielectric loss spectra (Figure 4d) where the peak location at equivalent temperatures was observed at higher frequencies. These observations all derive from the higher level of phase segregation in this system compared to the other gradient copolymers, as suggested also by DSC (Figure 1b) and the DRS isochronal representation in (Figure 2b), such that the relaxation time corresponds to regions richer in nBA relative to that predicted by the cumulative styrene composition.

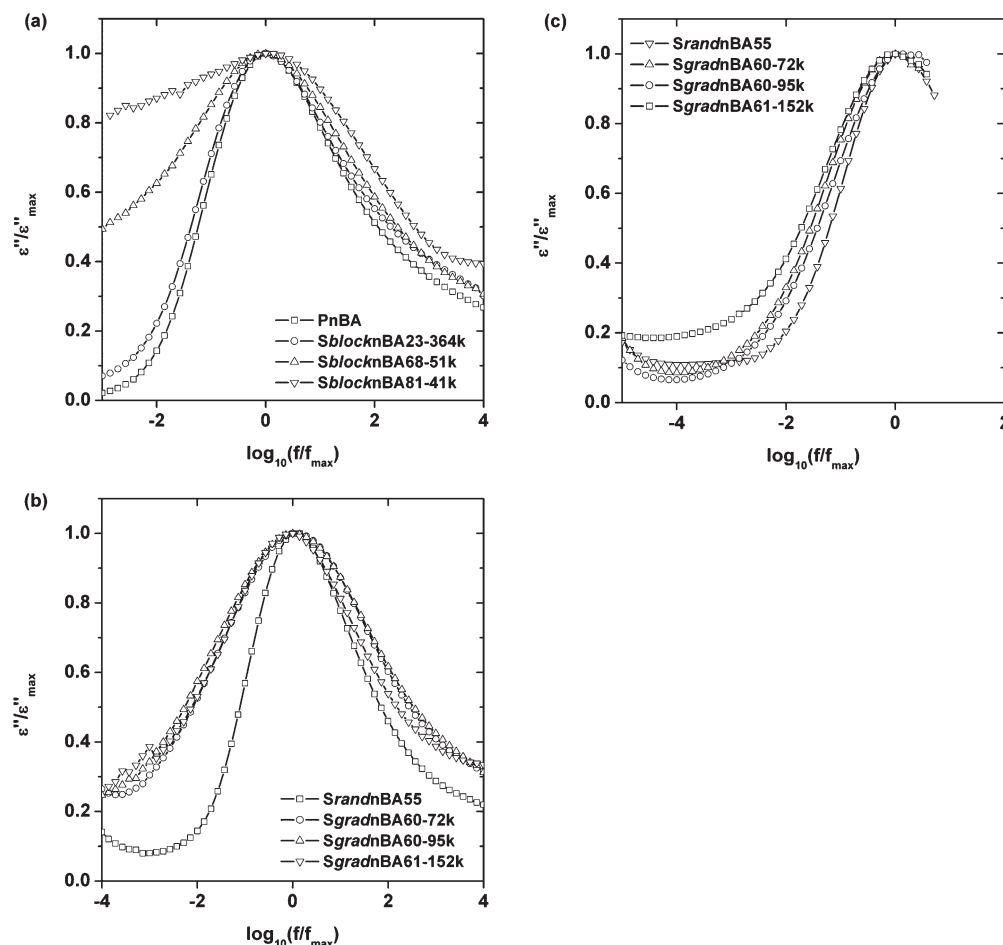


Figure 6. Dielectric loss spectra normalized by ϵ''_{\max} and f_{\max} at the temperature where f_{\max} of the segmental process was closest to 100 Hz for (a) PnBA (−30 °C), S-block-nBA23–364K (−30 °C), S-block-nBA68–51K (−25 °C) and S-block-nBA81–41K (−30 °C) and (b) for S-rand-nBA55 (50 °C), S-grad-nBA60–72K (45 °C), S-grad-nBA50–95K (45 °C) and S-grad-nBA61–152K (30 °C). Solid lines serve as a guide for the eye. (c) Normalized data where f_{\max} of the segmental process was closest to 1 MHz for S-rand-nBA55 (85 °C), S-grad-nBA60–72K (90 °C), S-grad-nBA50–95K (90 °C), and S-grad-nBA61–152K (70 °C).

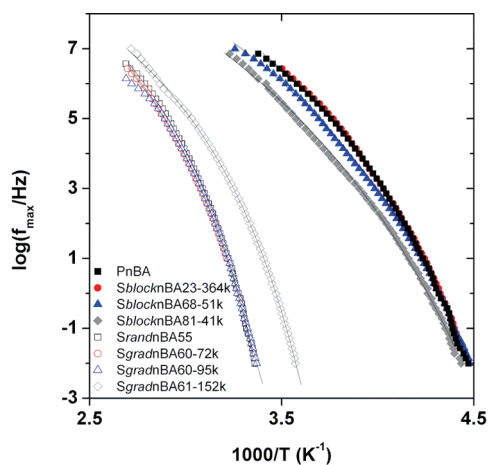


Figure 7. Positions of maxima characterizing segmental processes of PnBA and all S/nBA copolymers plotted as $\log(f_{\max})$ vs $1000/T$. Solid lines indicate VFT fits.

The segmental relaxation times were fit to the Vogel–Fulcher–Tammann (VFT) relation:⁶⁷

$$\tau_{\max} = \tau_0 \exp[B/(T - T_0)] \quad (2)$$

where τ_{\max} is the peak relaxation time, $\tau_0 = 1/(2\pi f_0)$ is a microscopic time scale for the α -process, B is an adjustable

Table 2. VFT Fit Parameters

| sample | $\log(f_0)$ (f_0 in Hz) | B (K) | T_0 (K) |
|--------------------|----------------------------|---------|-----------|
| PnBA | 13.0 | 1670 | 176 |
| S-block-nBA23–364K | 13.0 | 1660 | 176 |
| S-block-nBA68–51K | 13.3 | 1990 | 166 |
| S-block-nBA81–41K | 13.4 | 2270 | 161 |
| S-rand-nBA55 | 12.4 | 1640 | 248 |
| S-grad-nBA60–72K | 12.4 | 1690 | 246 |
| S-grad-nBA60–95K | 12.7 | 1820 | 243 |
| S-grad-nBA61–152K | 11.9 | 1580 | 230 |

parameter related to the activation energy and T_0 is the Vogel temperature. The fitted parameters are listed in Table 2.

The τ_0 and B values for all the segmental relaxations associated with the nBA rich phase are similar across all samples, with $\log(f_0) \sim 12$ –13 (consistent with “typical” values for $\log(f_0)$ ⁶⁴ and the expected time scale for α -relaxations) and $B \sim 1600$ –2300 K. We compare these to data previously reported in the literature for PnBA VFT and Williams–Landel–Ferry (WLF) parameters, where the WLF parameters c_1 and c_2 are related to VFT parameters through the substitutions described by Ferry:⁶⁸

$$c_1 = \frac{B}{2.303(T_r - T_0)} \quad (3)$$

$$c_2 = T_r - T_0 \quad (4)$$

Table 3. Havriliak–Negami Breadth and Shape Parameters

| sample | $T_f = 100\text{Hz}$ ($^{\circ}\text{C}$) ^a | α | γ |
|--------------------|--|----------|----------|
| PnBA | −30 | 0.80 | 0.23 |
| S-block-nBA23–364K | −30 | 0.69 | 0.26 |
| S-block-nBA68–51K | −25 | 0.38 | 0.60 |
| S-block-nBA81–41K | −30 | 0.33 | 0.74 |
| S-rand-nBA55 | 50 | 0.70 | 0.36 |
| S-grad-nBA60–72K | 45 | 0.37 | 0.71 |
| S-grad-nBA60–95K | 45 | 0.36 | 0.68 |
| S-grad-nBA61–152K | 30 | 0.41 | 0.67 |

^a The temperature where f_{max} of the segmental process is closest to 100 Hz.

where T_r is the reference temperature (typically the glass transition temperature, T_g) at which the parameters are defined. Our value of 1670 K for B for PnBA is somewhat higher but of the same order as those reported by Fioretto et al.⁶⁹ (1280 K) and Liedermann⁷⁰ (1420 K). There has been one previous publication⁶³ of VFT parameters for S/nBA random copolymers; their fitted value of B for a random copolymer with 55% styrene was 1300 K, somewhat lower than our value fitted for S-rand-nBA55 (1640 K).

The T_o values for the different materials reflect expectations based on their T_g values (T_o is roughly equal to $T_g - 50$ K). In the PnBA and block copolymer series, the T_o values for PnBA and S-block-nBA23–364K are the same (176 K), but T_o shifts to lower temperatures for the two shorter block copolymer cases (166 and 161 K). In the random and gradient copolymer series, the random copolymer and two shorter gradient copolymers exhibit similar values of T_o (243–248 K), while T_o associated with the nBA rich phase for S-grad-nBA61–152K is shifted to a lower temperature (223 K). The calculated value for T_o of PnBA (176 K) is in line with values previously reported in the literature.^{63,69}

3.4. Quantifying Heterogeneity: Havriliak–Negami Breadth and Shape Parameters. As a means of comparing dynamic heterogeneity, we examine the relaxation breadth parameters (α and γ from eq 1) from the Havriliak–Negami fits to the data (Table 3). These were taken from the temperature where f_{max} of the segmental process was closest to 100 Hz (also included in Table 3). The values of α and γ can vary between 0 and 1, with higher values corresponding to narrower and more symmetric relaxations (a narrower distribution of relaxation times). In keeping with Figure 5a, the breadth parameters for the PnBA and block copolymer series decrease from $\alpha = 0.80$ and $\gamma = 0.23$ for PnBA to $\alpha = 0.33$ and $\gamma = 0.74$ for the lowest molecular weight block copolymer. In the series composed of the random and gradient copolymers, the random copolymer exhibits the narrowest relaxation ($\alpha = 0.70$, $\gamma = 0.36$), very close to that measured for the PnBA homopolymer. Those for the two lower molecular weight gradient copolymers are much lower, with $\alpha = 0.37$ and $\gamma = 0.71$ for S-grad-nBA60–72K and $\alpha = 0.36$ and $\gamma = 0.68$ for S-grad-nBA60–95K; this reflects their broadened spectra observed in Figure 6(b) and their broader relaxation time distribution. As noted in Section 3.2, the α process of the nBA-rich phase for S-grad-nBA61–152K is slightly narrower than the lower molecular weight cases, and this is reflected in its slightly higher fitted value of $\alpha = 0.41$ (and $\gamma = 0.67$).

4. Conclusions

The block and gradient copolymer series display distinct segmental relaxation behavior. The segmental relaxation associated with the nBA regions of the block copolymers resembles that of PnBA but the relaxation becomes broader as the system shifts from highly to moderately segregated. Meanwhile, the gradient copolymer α relaxations largely resemble that of a

random copolymer with similar composition, but with broader relaxation time distributions. The one exception is S-grad-nBA61–152K, the most phase-segregated of the gradient copolymers, which exhibits contributions from a very wide range of compositions. Its overall segmental relaxation can be described as two overlapping contributions, representing regions of high nBA content and low nBA content. The Arrhenius plots of the α process of the nBA rich component reflects this picture, as the data corresponding to this peak fall at higher values of $1000/T$ than the other gradient copolymers and the random copolymer. The breadth in relaxation time achieved by this gradient copolymer reflects previous measurements of exceptional breadth as measured by DSC and is comparable to or exceeds that of a weakly segregated block copolymer.

Acknowledgment. We thank Prof. SonBinh Nguyen and Dr. Christine Dettmer (Northwestern University Chemistry Dept.) for synthesis of the initiator employed in three of our controlled radical copolymerization reactions. This work was funded in part by Northwestern University and the NSF-MRSEC program (Grant DMR-0520513) at the Materials Research Center of Northwestern University. The support of an Intel Ph.D. Fellowship and a Cabell Terminal Year Fellowship (to MMM) are gratefully acknowledged. KAM and JR would like to express their appreciation to the National Science Foundation, Polymer Program (DMR-0907139) for support of this research.

References and Notes

- (1) Pakula, T.; Matyjaszewski, K. *Macromol. Theory Simul.* **1996**, *5*, 987–1006.
- (2) Matyjaszewski, K.; Ziegler, M. J.; Arehart, S. V.; Greszt, D.; Pakula, T. *J. Phys. Org. Chem.* **2000**, *13*, 775–786.
- (3) Mok, M. M.; Pujari, S.; Burghardt, W. R.; Dettmer, C. M.; Nguyen, S. T.; Ellison, C. J.; Torkelson, J. M. *Macromolecules* **2008**, *41*, 5818–5829.
- (4) Lefebvre, M. D.; Olvera de la Cruz, M.; Shull, K. R. *Macromolecules* **2004**, *37*, 1118–1123.
- (5) Jiang, R.; Jin, Q. H.; Li, B. H.; Ding, D. T.; Wickham, R. A.; Shi, A. C. *Macromolecules* **2008**, *41*, 5457–5465.
- (6) Gray, M. K.; Zhou, H. Y.; Nguyen, S. T.; Torkelson, J. M. *Polymer* **2004**, *45*, 4777–4786.
- (7) Gray, M. K.; Zhou, H. Y.; Nguyen, S. T.; Torkelson, J. M. *Macromolecules* **2004**, *37*, 5586–5595.
- (8) Karaky, K.; Billon, L.; Pouchan, C.; Desbrières, J. *Macromolecules* **2007**, *40*, 458–464.
- (9) Jakubowski, W.; Juhari, A.; Best, A.; Koynov, K.; Pakula, T.; Matyjaszewski, K. *Polymer* **2008**, *49*, 1567–1578.
- (10) Paris, R.; De la Fuente, J. L. *J. Polym. Sci., Part B: Polym. Phys.* **2007**, *45*, 1845–1855.
- (11) Sun, X. Y.; Luo, Y. W.; Wang, R.; Li, B. G.; Zhu, S. P. *AIChE J.* **2008**, *54*, 1073–1087.
- (12) Kim, J.; Mok, M. M.; Sandoval, R. W.; Woo, D. J.; Torkelson, J. M. *Macromolecules* **2006**, *39*, 6152–6160.
- (13) Wong, C. L. H.; Kim, J.; Torkelson, J. M. *J. Polym. Sci., Part B: Polym. Phys.* **2007**, *45*, 2842–2849.
- (14) Mok, M. M.; Kim, J.; Wong, C. L. H.; Marrou, S. R.; Woo, D.; Dettmer, C. M.; Nguyen, S. T.; Ellison, C. J.; Shull, K. R.; Torkelson, J. M. *Macromolecules* **2009**, *42*, 7863–7876.
- (15) Karaky, K.; Péré, E.; Pouchan, C.; Desbrières, J.; Déral, C.; Billon, L. *Soft Matter* **2006**, *2*, 770–778.
- (16) Mok, M. M.; Kim, J.; Torkelson, J. M. *J. Polym. Sci., Part B: Polym. Phys.* **2008**, *46*, 48–58.
- (17) Mok, M. M.; Kim, J.; Marrou, S. R.; Torkelson, J. M. *Eur. Phys. J. E* **2010**, *31*, 239–252.
- (18) Williams, G. *Macromol. Symp.* **2009**, *286*, 1–19.
- (19) McCrum, N. G.; Read, B. E.; Williams, G. *Anelastic and Dielectric Effects in Polymeric Solids*; Dover Publications Inc.: New York, 1991.
- (20) Runt, J.; Fitzgerald, J. J. *Dielectric Spectroscopy of Polymeric Materials: Fundamentals and Applications*; American Chemical Society: Washington, DC, 1997.
- (21) Kremer, F.; Schönhals, A. *Broadband Dielectric Spectroscopy*; Springer-Verlag: Berlin, 2003.
- (22) Jin, X.; Zhang, S.; Runt, J. *Macromolecules* **2003**, *36*, 8033–8039.

- (23) Katana, G.; Fischer, E. W.; Hack, Th.; Abetz, V.; Kremer, F. *Macromolecules* **1995**, *28*, 2714–2722.
- (24) Miura, N.; MacKnight, W. J.; Matsuoka, S.; Karasz, F. E. *Polymer* **2001**, *42*, 6129–6140.
- (25) Zhang, S.; Painter, P. C.; Runt, J. *Macromolecules* **2004**, *37*, 2636–2641.
- (26) Wetton, R. E.; MacKnight, W. J.; Fried, J. R.; Karasz, F. E. *Macromolecules* **1978**, *11*, 158–165.
- (27) Fischer, E. W.; Zetsche, A. *Polym. Prepr.* **1992**, *203*, 117.
- (28) Fischer, E. W.; Zetsche, A. *Acta Polym.* **1994**, *45*, 168–175.
- (29) Simon, G. P.; Schonhals, A. In *Polymer Characterization Techniques and their Application to Polymer Blends*; Simon, G. P., Ed.; Oxford University Press: New York, 2003; Ch. 4.
- (30) Berzosa, A. E.; Ribelles, J. L. G.; Kripotou, S.; Pissis, P. *Macromolecules* **2004**, *37*, 6472–6479.
- (31) Atorngitjawan, P.; Klein, R.; McDermott, A.; Masser, K. A.; Painter, P.; Runt, J. *Polymer* **2009**, *50*, 2424–2435.
- (32) Lodge, T. P.; McLeish, T. C. B. *Macromolecules* **2000**, *33*, 5278–5284.
- (33) Lodge, T. P.; Wood, E. R.; Haley, J. C. *J. Polym. Sci., Part B: Polym. Phys.* **2006**, *44*, 756–763.
- (34) Alig, I.; Kremer, F.; Fytas, G.; Roovers, J. *Macromolecules* **1992**, *25*, 5277–5282.
- (35) Karatasos, K.; Anastasiadis, S. H.; Semenov, A. N.; Fytas, G.; Pitsikalis, M.; Hadjichristidis, N. *Macromolecules* **1994**, *27*, 3543–3552.
- (36) Karatasos, K.; Anastasiadis, S. H.; Floudas, G.; Fytas, G.; Pispas, S.; Hadjichristidis, N.; Pakula, T. *Macromolecules* **1996**, *29*, 1326–1336.
- (37) Watanabe, H. *Macromolecules* **1995**, *28*, 5006–5011.
- (38) Alig, I.; Floudas, G.; Avgeropoulos, A.; Hadjichristidis, N. *Macromolecules* **1997**, *30*, 5004–5011.
- (39) Floudas, G.; Paraskeva, S.; Hadjichristidis, N.; Fytas, G.; Chu, B.; Semenov, A. N. *J. Chem. Phys.* **1997**, *107*, 5502–5509.
- (40) Floudas, G.; Alig, I.; Avgeropoulos, A.; Hadjichristidis, N. *J. Non-Cryst. Solids* **1998**, *235–237*, 485–490.
- (41) Kawana, S.; Jones, R. A. L. *Phys. Rev. E* **2001**, *63*, 021501.
- (42) Kawana, S.; Jones, R. A. L. *Eur. Phys. J. E* **2003**, *10*, 223–230.
- (43) Ellison, C. J.; Torkelson, J. M. *Nat. Mater.* **2003**, *2*, 695–700.
- (44) Priestley, R. D.; Ellison, C. J.; Broadbelt, L. J.; Torkelson, J. M. *Science* **2005**, *309*, 456–459.
- (45) Rittigstein, P.; Torkelson, J. M. *J. Polym. Sci., Part B: Polym. Phys.* **2006**, *44*, 2935–2943.
- (46) Rittigstein, P.; Priestley, R. D.; Broadbelt, L. J.; Torkelson, J. M. *Nat. Mater.* **2007**, *6*, 278–282.
- (47) Fukao, K.; Miyamoto, Y. *Europhys. Lett.* **1999**, *46*, 649–654.
- (48) Fukao, K.; Miyamoto, Y. *Phys. Rev. E* **2000**, *61*, 1743–1754.
- (49) Priestley, R. D.; Broadbelt, L. J.; Torkelson, J. M.; Fukao, K. *Phys. Rev. E* **2007**, *75*, 061806.
- (50) Priestley, R. D.; Rittigstein, P.; Broadbelt, L. J.; Fukao, K.; Torkelson, J. M. *J. Phys. Cond. Matter* **2007**, *19*, 205120.
- (51) Serghei, A.; Kremer, F. *Phys. Rev. Lett.* **2003**, *92*, 165702.
- (52) Nicolas, J.; Ruzette, A. V.; Farcet, C.; Gérard, P.; Magnet, S.; Charleux, B. *Macromolecules* **2007**, *40*, 7029–7040.
- (53) Rana, D.; Bag, K.; Bhattacharyya, S. N.; Mandal, B. M. *J. Polym. Sci., Part B: Polym. Phys.* **2000**, *38*, 369–375.
- (54) Lessard, B.; Maric, M. *Macromolecules* **2008**, *41*, 7881–7891.
- (55) Lessard, B.; Tervo, C.; Maric, M. *Macromol. Reaction Eng.* **2009**, *3*, 245–256.
- (56) Eggenhuisen, T. M.; Becer, C. R.; Fijten, M. W. M.; Eckardt, R.; Hoogenboom, R.; Schubert, U. S. *Macromolecules* **2008**, *41*, 5132–5140.
- (57) Dire, C.; Belleney, J.; Nicolas, J.; Bertin, D.; Magnet, S.; Charleux, B. *J. Polym. Sci., Part A: Polym. Chem.* **2008**, *46*, 6333–6345.
- (58) Benoit, D.; Chaplinski, V.; Braslau, R.; Hawker, C. J. *J. Am. Chem. Soc.* **1999**, *121*, 3904–3920.
- (59) Havriliak, S.; Negami, S. *J. Polym. Sci., Polym. Symp.* **1966**, *14*, 99.
- (60) Miwa, Y.; Usami, K.; Yamamoto, K.; Sakaguchi, M.; Sakai, M.; Shimada, S. *Macromolecules* **2005**, *38*, 2355–2361.
- (61) Cervený, S.; Alegria, A.; Colmenero, J. *Phys. Rev. E* **2008**, *77*, 031803.
- (62) Fragiadakis, D.; Runt, J. *Macromolecules* **2010**, *43*, 1028.
- (63) Fitzgerald, J. J.; Binga, T. D.; Sorriero, L. J.; O'Reilly, J. M. *Macromolecules* **1995**, *28*, 7401–7406.
- (64) Ribelles, J. L. G.; Duenas, J. M. M.; Pradas, M. M. *J. Appl. Polym. Sci.* **1989**, *38*, 1145–1157.
- (65) Hayakawa, T.; Adachi, K. *Polym. J.* **2000**, *32*, 845–848.
- (66) Gaborieau, M.; Graf, R.; Kahle, S.; Pakula, T.; Spiess, H. W. *Macromolecules* **2007**, *40*, 6249–6256.
- (67) Hiemenz, P. C.; Lodge, T. P. In *Polymer Chemistry*; CRC Press: Boca Raton, FL, 2007.
- (68) Ferry, J. D. In *Viscoelastic Properties of Polymers*; John Wiley & Sons, Inc.: New York, 1980.
- (69) Fioretto, D.; Livi, A.; Rolla, P. A.; Socino, G.; Verdini, L. *J. Phys.: Condens. Matter* **1994**, *6*, 5295–5302.
- (70) Liedermann, K. *Colloid Polym. Sci.* **1996**, *274*, 20–26.